Catalysis Science & Technology

Accepted Manuscript

ROYAL SOCIETY OF CHEMISTRY

www.rsc.org/catalysis

Catalysis Science &Technology RSCPublishing

ARTICLE

Oxidation of Methanol to Methyl Formate over supported Pd nanoparticles: insights into the reaction mechanism at low temperature.

Cite this: DOI: 10.1039/x0xx00000x

Received 00th January 2012,
Accepted 00th January 2012

DOI: 10.1039/x0xx00000x

www.rsc.org/

R. Wojcieszak,[a,b,c*], A. Karelovic[a], E. M. Gaigneaux[a] and P. Ruiz[a]

Pd nanoparticles supported on TiO_2 and SiO_2 (2 wt.%) were synthesized by the water-in-oil microemulsion method. Material was characterized by standard physico-chemical methods (XRD, ICP, TEM, BET, XPS), DRIFT in *operando* mode and tested in gas-phase reaction of oxidation of methanol. The direct formation of methyl formate (MF) from methanol was observed. Supported palladium catalysts produced methyl formate at low temperature (< 100°C) with high selectivity. At higher temperatures methyl formate is not formed anymore and the total oxidation to CO_2 occurred. DRIFT-*operando* study confirmed that methanol is adsorbed mainly in two forms, the un-dissociated gaseous methanol (*via* H bond) and dissociatively adsorbed methoxy species (CH_3O^-) on the surface. Methyl formate is formed already at RT with the maximum at about 80°C. Mechanism of the formation of methyl formate from methanol at low temperature is discussed.

1. Introduction.

Aerobic oxidation of methanol at low temperature and atmospheric pressure is one of viable green routes to produce methyl formate. The catalytic properties of supported Pd nanoparticles in methanol oxidation reaction have been studied in the past years [1-4]. It was shown that this reaction may lead to different products such as formaldehyde (HCHO, FA), dimethoxymethane ($CH_3OCH_2OCH_3$, DMM), methyl formate ($HCOOCH_3$, MF) or to hydrogen. From the literature appears that oxidative routes to HCHO are involved on silver and iron molybdate catalysts. DMM could be produced using zeolites in a one step catalytic process [5]. Methanol can produce also hydrogen. It was shown that it can be produced using Cu/ZnO [6] and Cu/Zn/Al [7-8] catalysts.

Methyl formate, one of the important chemical intermediates used for the production of formamide, dimethylformamide, acetic acid, pharmaceuticals, fumigants and larvicides, can be produced via CH_3OH dehydrogenation on CuO [9] or Pd supported nanoparticles [2-4]. MF is industrially produced by reacting liquid methanol with dry gaseous CO under high pressure, 2–4 MPa, and temperatures between 50–150°C over a potassium/sodium alkoxide catalyst [10].

An important aspect in methanol oxidation is the reaction temperature. Previously, using palladium nanoparticles of different sizes (1-8 nm) supported on TiO_2 (2 wt.%) the direct formation of methyl formate from methanol in presence of oxygen was observed. It was demonstrated that supported palladium catalysts produced methyl formate but at low temperature (<100 °C) with a very high selectivity. At higher temperature, methyl formate was not formed at all and the total oxidation to CO_2 occurred [2]. These observations had not been reported previously in the literature. In addition, it was also demonstrated that in the oxidation of methanol at low temperature the size of Pd supported nanoparticles is crucial for the formation of methyl formate. There is a correlation of the average palladium particle sizes with the methyl formate yield. The highest conversion was observed for the smallest palladium particles (1.3 nm). The lowest conversion was observed for the biggest particles (5.9 nm). This catalyst also showed the highest selectivity to methyl formate (100%) and no CO_2 was formed at 50°C. indicating that for this reaction, the control of the size of Pd particles is important.

The mechanism resulting in methyl formate formation from methanol involves a C-O-C coupling [1-5]. Meanwhile, there is still no consensus on the role of the nature of the active phase and on the mechanism of the reaction. It was claimed in the literature that MF can form via different pathways: *i)* condensation of adsorbed methoxides with HCHO to form methoxymethanol intermediates (CH_3OCH_2OH) that then dehydrogenate to MF [11], *ii)* esterification of formic acid (HCOOH) intermediates formed by HCHO oxidation or *iii)* HCHO dimerization [11-12]. But these mechanisms were obtained under more drastic reaction conditions (200-300°C) and with different catalysts (Ag (110), $CuSiO_2$, SnO_2-MoO_3) [11-13].

The objective of this work is to clarify which reaction intermediates are involved in the mechanism of methanol oxidation at low temperature over Pd supported nanoparticles. This information is important to compare with the mechanisms proposed at higher temperature and to design more active catalysts working at lower temperature. For that, *in situ* DRIFT study coupled with a mass spectrometry was used to investigate the nature of the adsorbed species from methanol, the intermediate species formed and the reactivity of these species.
In this study catalysts having a very narrow distribution of the size of Pd nanoparticles were synthesized. Palladium nanoparticles were prepared using the water-in-oil microemulsion method, which permitted to control final size of the Pd particles accurately [3-4]. To enlarge the knowledge of the system, SiO_2 was used also as support.
Catalysts were also characterized using several physico-chemical methods (ICP, N_2 BET, H_2 chemisorption, XRD, XPS, TEM). The results shown here could provide insight on the intermediate of the reaction and on its reactivity at low temperatures (50-80°C).

2. Experimental

2.1 Catalysts preparation

Palladium (II) chloride (from Aldrich) was used as the Pd precursor and TiO_2 (Merck, BET: 8 m^2g^{-1}) and SiO_2 (Chempur, BET: 14 m^2g^{-1}) as the supports. The organic surfactant used was sodium bis(2-ethylhexyl)sulfocuccinate (AOT), Sigma Aldrich, purity 96%. Organic solvent was cyclohexane (Fluka purity 99.5%). Hydrazine hydrate solution (Fluka, 80%). All reagents were used without further purification.

Catalyst was prepared as follows. i) *precursor solution:* the appropriate quantity of $PdCl_2$ was dissolved in 5 ml of distilled water in the presence of NaCl (Merck, 99.5%). Then the solution was evaporated at 60°C until only a volume of 1 ml remained, ii) *microemulsion:* it was formed using 50 ml of cyclohexane, 1 ml of precursor solution and the appropriate quantity (6.25 g) of AOT. The microemulsion was then heated to 50°C and then 2 g of support were incorporated to the reactant flask under magnetic stirring. After 30 minutes the 3 ml of hydrazine was injected. The reduction by hydrazine was carried out in a thermostated water bath at 50°C. The time of reduction of 30 min was measured from the hydrazine addition to the microemulsion. The reduction was carried out under nitrogen atmosphere. The reactant solution changed colour from light red to black indicated the reduction of palladium. The solution was then filtered, washed with acetone (VWR, 99%) and distilled water for 1h and drying at 100 °C for 30 minutes.

To compare with the catalysts, the bare oxides (2 g of TiO_2 and SiO_2) were also treated with hydrazine in the same conditions as the catalysts, using the same amounts of NaCl, water, cyclohexane and AOT. These supports were denoted as TiO_2-N_2H_4 and SiO_2-N_2H_4.

2.2. Characterization of physical and chemical properties

2.2.1. Chemical Analysis

ICP-AES (Inductively Coupled Plasma-Atomic Emission Spectroscopy) analysis was used to determine the chemical composition of the prepared catalysts and was performed on a Thermo Jarrel ASH IRIS Advantage analyzer.

2.2.2. X-ray Diffraction

X-ray diffraction study was carried out on a Bruker D8 DISCOVER diffractometer using the Kα radiation of Cu (1.5418 Å). The 2Θ range was scanned between 10 and 60° at a rate of 0.01 $degree_*s^{-1}$. The identification of the phases was achieved by using the ICDD-JCPDS database.

2.2.3.N_2 physisorption

The textural properties of the support and reduced materials were studied by means of N_2 adsorption/desorption at -196°C with a Micromeritics ASAP2000 apparatus. Low temperature nitrogen adsorption isotherms enable the BET calculation of the specific surface area, and the BJH calculation of the pore volume and the pore diameter.

2.2.4. X-ray photoelectron spectroscopy

XPS analyses were performed on an SSI X-probe (SSX-100/206) spectrometer from Surface Science Instruments. The analysis chamber was operated under ultrahigh vacuum with a pressure close to $5*10^{-9}$ Torr and the sample was irradiated with a monochromatic Al Kα (1486.6 eV) radiation (10 kV; 22 mA). Charge compensation was achieved by using an electron flood gun adjusted at 8 eV and placing a nickel grid 3.0mm above the sample. The analysed area was approximately 1.4 mm^2 and the pass energy was set at 50 eV for recording high-resolution peaks. In these conditions, the full width at half maximum (FWHM) of the Au $4f_{7/2}$ peak of a clean gold standard sample was about 1.1 eV. For these measurements, the binding energy (BE) values were referred to the C-(C,H) contribution of the C 1s peak at 284.8 eV. The surface atomic concentrations were calculated by correcting the intensities with theoretical sensitivity factors based on Scofield cross-sections [14]. Peak decomposition was performed using curves with an 85% Gaussian type and a 15% Lorentzian type, and a Shirley non-linear sigmoid-type baseline. The following peaks were used for the quantitative analysis: O 1s, C 1s, Ti 2p, Si 2p, N1s and Pd 3d. Based on the XPS analysis, the XPS surface ratio of a given element is defined as the atomic concentration of the element (%) divided by the atomic concentration of Ti (%) or Si (%). XPS was also used for the determination of average Pd particle size using method described in [15-16].

2.2.5. Electron microscopy

Transmission electron microscope (TEM) micrographs were recorded on a LEO 922 Omega transmission electron microscope at an accelerating voltage of 200 kV after placing a

drop of the catalyst suspension on a carbon coated copper grid. The samples were removed from the reactor and stored in small glass containers until TEM inspection. The catalyst suspension was obtained by ultrasonically dispersing the sample in 1-butanol.

2.3. DRIFT study

In situ Diffuse Reflectance Infrared Fourier Transform Spectroscopy (in situ DRIFTS) spectra were collected on a Bruker Equinox 55 infrared spectrometer equipped with an air-cooled MIR source with KBr optics and a MCT detector. Spectra were obtained by collecting 200 scans with a resolution of 4 cm^{-1}. Samples were placed without packing or dilution inside a cell with controlled temperature and environment reflectance (Spectra-Tech 0030-102) with ZnSe windows, which was coupled to the spectrometer (Scheme 1). Standard FTIR spectra of the catalysts were carried out on a Bruker spectrometer equipped with a microplate module HTS-XT.

DRIFT Procedure

Samples were treated in situ at 400 °C with H_2 (Praxair, 99%)/He (Praxair, 99%) mixture (10% vol. of H_2, ramp: 5 °C min^{-1}, flow: 30 cm^3 min^{-1}). After that, the sample was cooled down under He and purged with He for 1h at RT. A reactant gas mixture containing 5 vol. % of methanol and 2.5 vol. % of O_2, was prepared by passage of a He stream through methanol (Merck, >99%) placed in a saturator maintained at 5.4 °C. The reactant mixture was passed through the DRIFT reacting cell with a total flow rate of 30 cm^3 min^{-1}. The experiments were carried out at various temperatures (25, 80, 100, 125, 150, 200, 225, 250 and 300 °C). The sample was heated or cooled at a rate of 10°C$*min^{-1}$. The gases at the outlet of the cell were analyzed by a quadrupole mass spectrometer (Balzers QMS 200) by following the evolution of the *m/z* = 2 (H_2), 15 (CH_4), 18 (H_2O), 28 (CO) and 44 (CO_2), 31 (CH_3OH), and 60 ($CHOOCH_3$).

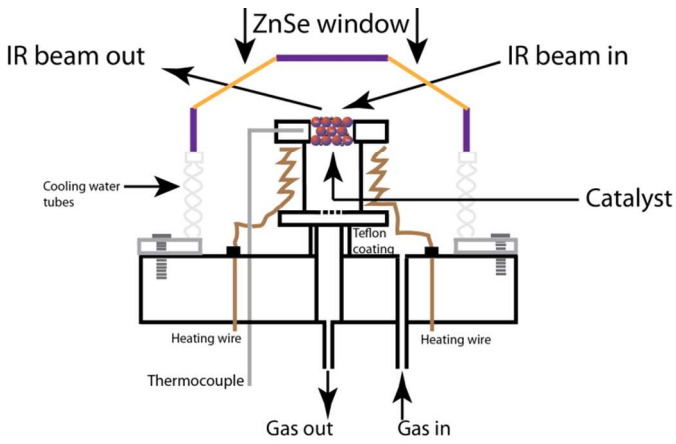

Scheme 1. Schematic representation of the experimental DRIFT-*operando* reactor used in this study.

For methanol absorption experiments, the sample was treated in situ at 400 °C with H_2 (Praxair, 99%)/He (Praxair, 99%) mixture (10% vol. of H_2, ramp: 5 °C min^{-1}, flow: 30 cm^3 min^{-1}). After that, the sample was cooled down under He and purged with He for 1h at RT. The methanol (5 vol. %/He) mixture was passed through the DRIFT reacting cell with a total flow rate of 30 cm^3 min^{-1}. At each temperature the evacuation under He was performed.

2.4. Catalytic test

The reaction of partial oxidation of methanol (POMeOH) was performed in a metallic fixed-bed microreactor made of an inconel tube of 1cm internal diameter (PID ENG&Tech, Madrid, Spain), operating at atmospheric pressure. The catalytic bed was composed of 100 mg of catalyst powder selected within the granular fraction of 200–315 μm and diluted in 600mg glass spheres that was confirmed inactive. The catalyst was placed in the reactor. Before the catalytic test, catalysts was treated in a flow of pure hydrogen (Praxair, 99 % flow rate = 50 cm^3 min^{-1}) at 300°C for 1h and heating with a ramp of 10°C min^{-1}, then the sample was cooled to 300°C. After the reduction, a gas mixture containing 5 vol. % of methanol (Merck, >99%) and 2.5 vol. % of O_2 (Praxair, 99%), was prepared by passage of a He stream through methanol placed in a saturator maintained at 5.4 °C. The reactant mixture was passed through the reactor with a total flow rate of 100 cm^3 min^{-1}. The standard catalytic test was carried out at various temperatures (75, 100, 125, 150, 200, 225, 250 and 300 °C). The sample was heated or cooled at a rate of 10°C min^{-1}. Methanol, oxygen and the reaction products were analyzed each 30 min using a CP3800 Varian gas chromatograph, operated at a programmed temperature and with a TCD detector. CP-Poraplot Q (25m*0.53mm) and CP-Molsieve 5A (25m*0.53mm) columns were used for separation of the reaction products. H_2, O_2, CH_4, CO, CO_2, methanol, methyl formate and H_2O were analysed during then reaction.

3. Results

3.1. ICP analysis, N_2 BET and XPS particle size determination.

The results of ICP analysis and BET surface area are given in Table 1. The mass content of Pd was between 1.8 and 1.9% which was smaller than the nominal expected (2 wt.%). BET surface area of the commercial supports was 8 and 14 m^2g^{-1} for TiO_2 and SiO_2 respectively In the case of Pd/TiO_2 catalyst the BET surface area did not change significantly after chemical reduction as showed by the BET results. On the contrary the BET surface area of Pd/SiO_2 samples decreased drastically to 5.6 m^2g^{-1}. Bare oxides treated with hydrazine in the same conditions as the catalysts show the same BET surface area of non treated oxides (8 and 13.8 m^2g^{-1}). In order to estimate the average palladium particle size the Davis model was applied using the intensity ratio of two dispersed phase core levels with different kinetic energy. The results are presented in Table 1. In this study, the two core levels used to determine the size of palladium particles are 3d with the binding energy about 334 eV and Auger $M_{45}N_{45}N_{45}$ peak at 1161 eV. In the case of

catalysts reduced by hydrazine the calculations confirmed the presence of the very small palladium particles with diameter of 1.3 for Pd/TiO_2 catalyst and 4.5 nm for Pd/SiO_2. Moreover, the sintering of the Pd particles was not observed after the catalytic test as calculated from XPS data (Table 1). Microemulsion method with AOT and cyclohexane mixture permitted to obtain very small particles in the case of Pd supported on TiO_2 oxide. In the case of SiO_2 supported catalysts Pd particles are bigger but still remain small. As expected microemulsion method allows to prepare small metallic nanoparticles, as described in the literature [17-18].

Table 1. ICP, BET and XPS results of fresh catalysts and after DRIFT study.

Sample	Pd[a] [wt.%]	Surface area[b] [m^2g^{-1}]	Particle size[c] [nm]
TiO_2	-	8.0	-
SiO_2	-	14.1	-
Pd/TiO_2	1.8	7.8	1.3 (1.3)[d]
Pd/SiO_2	1.9	5.6	4.5 (4.3)[d]
TiO_2-N_2H_4	-	8.0	-
SiO_2-N_2H_4	-	13.8	-

[a]from ICP, [b]from BET, [c]from XPS study, [d]average particle size after DRIFT test

3.2. Structural and morphological characteristics of palladium nanoparticles.

XRD analysis shows the presence of TiO_2 in anatase structure. XRD study of the catalyst indicated palladium in metallic state after hydrazine reduction (Figure 1). However, the very low resolution of these reflections did not allow determining the average particle size from the well-known line broadening analysis as proposed by Scherrer.

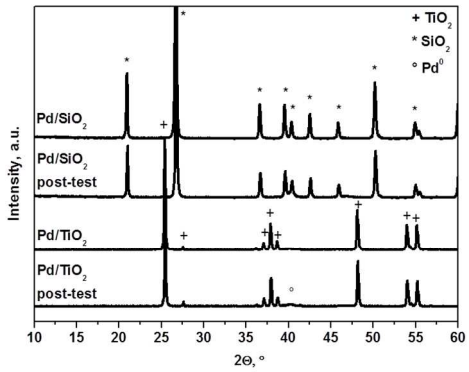

Figure 1. XRD patterns of the fresh and spent catalysts.

In the case of Pd/SiO_2 catalysts the XRD patterns showed only peaks originated from crystalline SiO_2 (Figure 1). As suggested XPS analysis, Pd particles sizes are very small and they cannot be detected by XRD technique. In the case of Pd/SiO_2 catalyst there is an overlapping of Pd and SiO_2 signals, which did not permit the particle size determination.

The palladium nanoparticles were not visible on TEM images for Pd/TiO_2 (Figure 2a). The palladium particles formed after the reduction with the hydrazine are very small (<2 nm) which confirms the results obtained by XPS (see Table 1).

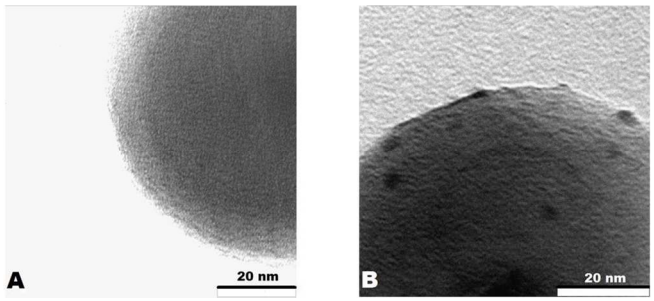

Figure 2. TEM images of fresh Pd/TiO_2 (A) and Pd/SiO_2 (B) catalysts

In the case of Pd/SiO_2 catalyst (Figure 2b) the TEM image showed small Pd particles of about 5 nm. This value was also confirmed by XPS study (Figure 3). As observed in TEM image, microemulsion method allows to obtain nanoparticles with a narrow size distribution, as indicated previously [2].

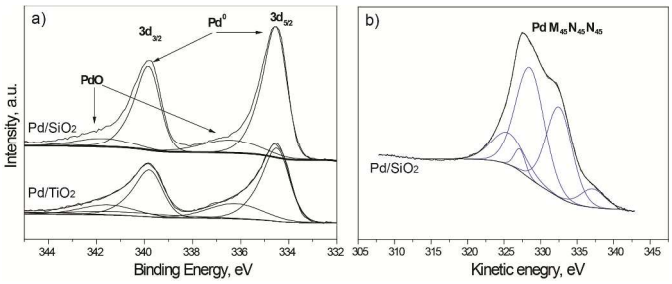

Figure 3. XPS Pd 3d region for fresh Pd/SiO_2 and Pd/TiO_2 catalysts (a) and Auger peak $M_{45}N_{45}N_{45}$ for Pd/SiO_2 sample (b)

3.3. Surface properties.

XPS study is able to determinate the chemical composition and oxidation degrees of components presents on the catalyst surface.

Table 2. XPS results of fresh catalysts and pure supports (after hydrazine treatment).

Sample	Pd^0 [%]	Pd^+ [%]	Pd^0/Pd^+	C 1s [%]
Pd/TiO_2	1.23	0.47	2.62	23.1
Pd/SiO_2	1.52	0.38	4.01	21.5
TiO_2	-	-	-	18.9
SiO_2	-	-	-	16.5
TiO_2-N_2H_4	-	-	-	21.3
SiO_2-N_2H_4	-	-	-	22.5

Palladium is not fully reduced. Palladium in metallic state (Pd^0) as well as oxidized palladium (Pd^+) were detected. The XPS Pd^0/Pd^+ atomic ratio confirmed the fact that palladium is principally reduced. Carbon (about 20%) was observed on the samples and it was similar in all samples. The results are given in the Table 2 and Figure 3.

3.4. Catalytic activity

During the catalytic tests only methyl formate, CO_2, CO and H_2O products were detected. Bare TiO_2 and SiO_2, and previously treated in aqueous hydrazine media (TiO_2-N_2H_4, SiO_2-N_2H_4), showed no activity in the oxidation of methanol at low temperature (below 150°C) (Table 3). Some activity was however observed at high temperature (above 150°C). The only product was CO_2 indicating the unselective complete oxidation of methanol.

Pd/SiO_2 catalyst showed the highest activity in the oxidation of methanol. Pd/TiO_2 catalyst is also highly active at low temperature (50-80 °C). Methyl formate was produced with a very high selectivity (about 82 % at 80°C) (Table 3). Only small amounts of CO_2 and H_2O, as secondary products, were observed. In 100-150°C temperature range, conversion of methanol was practically 100% for both samples and the selectivity decreases drastically (from 100 to 35 %).

At high temperature (>150°C), the conversion of methanol is complete, but methyl formate does not continue to be formed at all. The total methanol conversion was observed at above 150°C. Under these conditions, only CO_2 was observed. Traces of CO were observed at higher temperature (300°C).

Table 3. Catalytic results of gas phase oxidation of methanol.. Conversion of methanol (X),yield (MFY) and selectivity in methyl formate (MFS) X, conversion(%) for Pd/SiO_2, Pd/TiO_2 catalysts and SiO_2 and TiO_2 supports

catalysts	X [%]		MF Y[%]		MF S [%]	
	50°C	80°C	50°C	80°C	50°C	80°C
Pd/SiO_2	37	88	29	63	78 (22)[b]	72 (28)[b]
Pd/TiO_2	3	67	3	55	100 (0)[b]	82 (18)[b]
SiO_2[a]	0	0	0	0	0	0
TiO_2[a]	0	0	0	0	0	0

[a]hydrazine treated supports did not show any activity in methanol oxidation reaction, [b]in brackets selectivity to CO_2

3.5. DRIFT-*operando* results

Figure 4 shows the mass m/z=60 spectra collected during the methanol oxidation experiments on Pd/SiO_2 catalyst. No traces of formaldehyde or dimethoxymethane were observed.

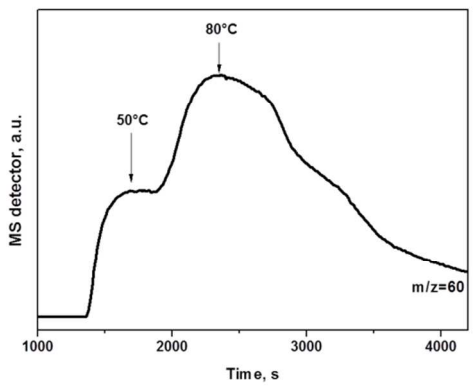

Figure 4. MS spectra of the m/z=60 (methyl formate)

The MF (m/=60) are produced already at RT with the maximum at about 80°C. The formation of MF strongly decreased at temperatures higher than 80°C (Figure 4).

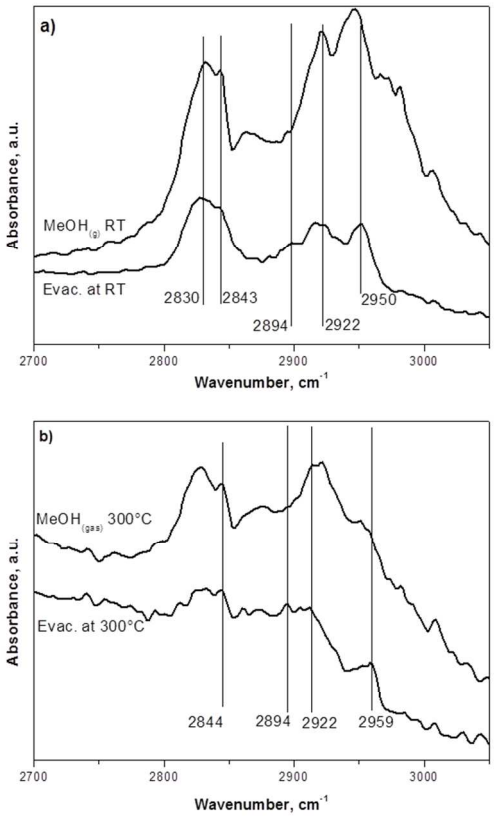

Figure 5. DRIFT results. Methanol adsorption (5 vol.% diluted in He) and evacuation with He, at RT (a) and at 300°C (b) over Pd/SiO_2 catalyst.

IR spectra of adsorbed methanol on Pd/SiO_2 at room temperature without oxygen are presented in Figure 5a. The spectra obtained after evacuation at RT and 300°C are presented in Figures 5a and 5b

respectively. The adsorption of methanol at RT resulted in the formation of several bands in the wavenumber regions: 3000-2800 cm^{-1} and 1000 cm^{-1}. At room temperature bands at 2830, 2843, 2894, 2922 and 2950 cm^{-1} were observed when methanol is adsorbed. After evacuation with He at RT, intensity of all bands strongly decreased. The resultant bands corresponding to the formation of methoxy species on the catalyst surface. The differences were observed after evacuation at 300°C. Only small bands at 2844 and 2959 cm^{-1} were observed.

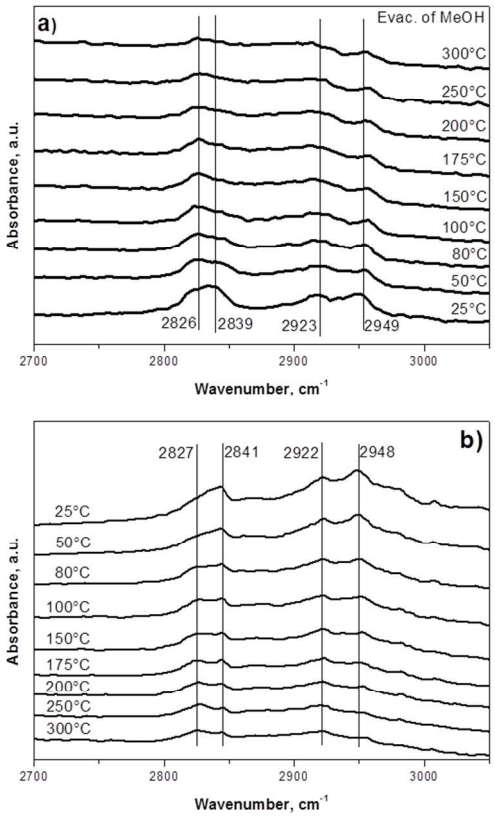

Figure 6. DRIFT spectra of the evacuation under He 30 ml/min after adsorption of methanol (5 ml/min) over Pd/TiO_2 catalyst at different temperatures a) and DRIFT spectra of the methanol oxidation reaction (5 vol. % of methanol and 2.5 vol. % of O_2) at different temperatures b)

Figures 6a and 6b present DRIFT spectra of the evacuation after adsorption of methanol over Pd/TiO_2 catalyst at different temperatures. Bands at 2950 , 2922, 2913, 2843 and 2830 cm^{-1} are observed. The bands at 2925 and 2820 cm^{-1} correspond to the methoxy species adsorbed on the surface of catalyst [19-21]. Bands localized at 2948 and 2841 cm^{-1} are originated from the gaseous methanol. All bands start to disappear after evacuation at RT and are removed completely after evacuation at 300°C (Figure 6a and 6b). They can be attributed to un-dissociated methanol weakly bounded via H-bond [19-20]. Contrary to that, the bands of methoxy species are present even after evacuation at 300°C (Figures 6a and 6b) confirmed a strong adsorption of these species on the surface [21]. Bands of methoxy species localized at 2922 cm^{-1} and 2827 cm^{-1} corresponded to the bond vibration of $\upsilon s(CH_3)$ and the Fermi resonance of $2\delta_s(CH_3)$, respectively, in the methoxy group [3,5,18]. During the catalytic test (5 vol. % of methanol and 2.5 vol. % of O_2) the additional bands start to appear at 1750 cm^{-1} and 1200 cm^{-1} already at about 25°C which are attributed to the methyl formate as shown in Figure 7. The increase of the intensity of these bands was observed at 50 and 80°C. Increase of the temperature up to 150°C resulted in the disappearance of these bands as shown in Figure 7. Additional bands (Figure 7) were observed at 1646, 1448, 1221 and 1057 cm^{-1} which correspond to the vibration of $\upsilon(C=O)$, $\delta(CH_2)$ and $\gamma(CH_2)$ in adsorbed formaldehyde [19-21]. No bands originated from methoxymethanol or dioxymethylene intermediates were observed.

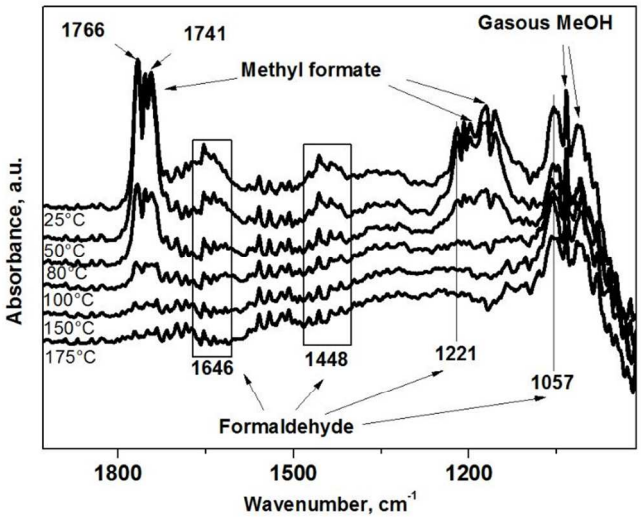

Figure 7. DRIFT-*operando* spectra under methanol oxidation (5 vol. % of methanol and 2.5 vol. % of O_2) over Pd/SiO_2 catalyst at different temperatures.

4. Discussion

4.1. Physical and chemical properties of the supported catalysts

The modification of titania support via Pd water-in-oil microemulsion method did not change the adsorption isotherm and the BET surface area practically remains unchanged. Any changes in the BET specific surface area were observed when the pure support was treated in the presence of N_2H_4. In addition, no changes in XPS spectra of fresh and hydrazine treated supports were observed. It could be concluded that hydrazine does not change the chemical state of titanium oxide support.

Contrary to that, significant changes in the specific surface area were observed in the case of Pd/SiO_2 catalyst. The BET surface area decreased two times. That could be due to the filling of the mouth of catalyst pores by Pd particles. But also the collapse of some pores could be expected due to the high pH of the preparation solution (pH=11).

The results obtained from XPS study using Davis model permitted to confirm the results obtained from XRD and TEM studies. After reduction with N_2H_2 very small Pd particles could be obtained (Table 1). For Pd/TiO_2 the palladium particles

formed after the reduction with the hydrazine are very small (<2 nm). For Pd/SiO_2 catalyst, Pd particles of about 5 nm were observed (TEM, XPS). Microemulsion method allows obtaining nanoparticles with a narrow size distribution. XPS study confirmed also the fact that in all catalysts palladium is not fully reduced (Table 3). The presence of the oxidized palladium on the surface could be explained by the diffusion of oxygen from the bulk of the palladium particles towards its surface. In fact an oxidized layer always forms on the surface of palladium, even after reduction with hydrogen. It was shown already that $Pd/\gamma\text{-}Al_2O_3$ catalyst is always in an oxide PdO form with its surface in an intermediate state between surface lacunary PdO and crystalline PdO species. This phenomenon has been demonstrated experimentally by Raman spectroscopy [22]. Part of the presence of the oxidized palladium could be due also to the air exposition under washing and drying steps, but it seems that if this is the case, this effect seems to be minimal. The XPS values of the Pd^0 to Pd^+ (Table 3) molar contributions give information about the reduction degree of the palladium before and after catalytic test. The increase of this ratio observed after catalytic test could be explained by the reducing role of methanol [2-4].

4.2. Catalytic activity

Pd/SiO_2 catalyst showed the highest activity in the oxidation of methanol at low temperature. Pd/TiO_2 catalyst is active preferentially from 80 °C. Methyl formate was produced with a very high selectivity (about 82 % at 80°C). Only small amounts of CO_2 and H_2O, as secondary products, were observed. For temperatures > 100° C conversion of methanol was practically 100% but the selectivity decreases drastically (less than 10%). As indicated in previous works, the results confirm that at high temperature (>150°C), the conversion of methanol is complete, but methyl formate it is not formed. At higher temperature (> 150°C) only CO_2 was observed. Taking into account the physicochemical characterization the difference in the catalytic activity between Pd/TiO_2 and Pd/SiO_2 could be related to the different amount of XPS Pd^0/Pd^+ atomic ratio. Pd supported on SiO_2 is more oxidized than Pd supported on TiO_2. But this effect is only important when the temperature is too low (80°C). At higher temperature, activity is more or less the same.

4.3. *In situ* DRIFT and mechanism of the reaction

Results give important indications to understand the mechanism of reaction at low temperature (< 100°C). The intensity of methoxy species bands (2922 and 2827 cm^{-1}) decreased slightly during the catalytic test (Figure 6b). This could be an indication that the methoxy species participate directly in the mechanism of methyl formate formation. It could be argued that the formation of new methoxy species is too fast to be seen during DRIFT analysis. The bands corresponding to gaseous methanol (2948 and 2841 cm^{-1}) also decreased during catalytic test. It could be suggested that gaseous methanol reacted directly to form methyl formate and/or adsorbed to form new methoxy species. The evacuation study of the adsorbed methanol (Figure 6a) shown that the methoxy species are present even at 300°C under He flow (without the methanol source). This suggests that methoxy species are strongly adsorbed on the surface. The decrease of the intensity of the bands corresponding only to the gaseous methanol (Figure 6b) suggests that it may react directly, without formation of methoxy species, to form methyl formate at low temperature and CO_2 at high temperature. The traces of formaldehyde were detected using mass spectrometry and IR studies. It could be concluded that

It has been suggested that the reaction resulting in methyl formate formation involves a C-O-C coupling. There is still no consensus on the role of the nature of the active phase, the role of the support and the reactant molecules, or the rate-determining step for this reaction. The only agreement that comes out from the literature data is that the surface reaction sequences change in a wide range with the reaction conditions. Methanol oxidation reactions lead to formaldehyde (HCHO), dimethoxymethane ($CH_3OCH_2OCH_3$, DMM), and methyl formate ($HCOOCH_3$, MF) products. Oxidative routes to HCHO are practiced on silver-based and iron-molybdate catalysts [11, 23]. Methyl formate, is produced *via* (non-oxidative) CH_3OH dehydrogenation on CuO or carbonylation using liquid bases [11, 24-25] and DMM can be produced in a two-step process involving methanol oxidation to HCHO followed by acetalization of $HCHO\text{-}CH_3OH$ mixtures with liquid or solid acids [11]. It was showed that the decomposition of methanol on TiO_2 starts with the formation of methoxide species upon the adsorption at room temperature [26]. On the TiO_2 surface the scission of both, C-O and O-H bonds is equally probable [26-27]. As postulated in the literature the reactivity changes in MeOH oxidation could be associated to the strength of the oxygen–metal bond of the reaction intermediates over metallic Pd clusters. Weakly bonded chemisorbed oxygen species would remove adsorbed hydrogen atoms formed during C-H activation steps of the reaction and, at the same time, would inhibit the total oxidation of the reaction intermediates to CO_2 [12].

It has been proposed that when methanol is adsorbed on the surface of Pd, its OH bond weakens, formation of Pd–O bonds prevails, chemisorbed methoxy species CH_3O^+ are formed, then undergoing successive dehydrogenation to formaldehyde CH_2O and then to chemisorbed CO and H [26]. It was shown, that in the case of Pd/SiO_2 catalysts the methanol adsorbs and reacts at 25°C on Pd and the dissociation of methanol via both O–H and C–O bond breaking is observed. At room temperature, adsorbed CH_3OH decomposes easily on the Pd crystallites, to give CO multicoordinated to the metal surface. Formyl species have also been found at this temperature, but they promptly disappear when the catalyst is heated and the formation of CO and H_2 prevails [24, 28]. The same was observed in our study. The formation of formaldehyde already at RT was confirmed by FTIR and mass spectrometry studies.

In our case it seems that methyl formate is formed rather *via* condensation of HCHO with gaseous methanol to form methyl formate than from the condensation of adsorbed methoxides with HCHO. This second mechanism should occur *via* the

formation of methoxymethanol intermediates (CH_3OCH_2OH), which then dehydrogenate to methyl formate [12]. However, in our case no bands originated from methoxymethanol were observed. In addition, the formation of formaldehyde was observed in mass spectrometry and FTIR studies. Literature suggests that the first reaction step would be the formation of methoxy groups by dissociative adsorption of methanol on a dual acid–base site formed by an accessible cation and a surface oxygen ion [23]. The methoxy species are further transformed to different intermediates depending on the acid strength of the site on which it is adsorbed and on the nature of the active centers in close proximity. It could be expected that desorption of the reaction products will be more favored by a weak than by a strong acid site [4, 23]. According to this scheme, the selective formation of formaldehyde and then methyl formate at low temperature would require both weak acidic and basic sites to limit the H abstraction and to prevent a very strong adsorption of formaldehyde. If the acid sites are too strong, the residence time of formaldehyde species is long enough to form a dioxymethylene species. If both acidic and basic sites are stronger than those needed for methyl formate formation, the intermediates would be further oxidized to carbon oxides [21, 23]. It could be concluded that at low temperature, adsorption of methanol produced surface methoxy species, which then dehydrogenated to form formaldehyde. The adsorbed formaldehyde reacts with gaseous methanol to form methyl formate. At higher temperature adsorbed methoxy species decompose into CO and/or CO_2.

Conclusions

The results obtained showed that catalysts prepared by microemulsion method are very active and selective in low temperature (<100°C) oxidation of methanol to methyl formate.

The mechanism of methyl formate formation from methanol *via* condensation of adsorbed HCHO with gaseous methanol was confirmed by DRIFT-*operando* study. The methoxy species strongly adsorbed on the surface seem to not participate directly in the mechanism. They need to be transformed into formaldehyde. Taking this into account the first reaction step would be the formation of methoxy groups by dissociative adsorption of methanol and then their transformation into formaldehyde. The formation of intermediate HCHO species was observed which confirmed this thesis. In the final step the adsorbed formaldehyde species would react with gaseous methanol to form methyl formate.

Acknowledgements

The authors acknowledge the Univeristé catholique de Louvain and the Fonds National de la Recherche Scientifique (FNRS) of Belgium. The authors involved in the "INANOMAT" IUAP network acknowledge the service Public Fédéral de Programmation Politique Scientifique (Belgium). The REALCAT platform is benefiting from a Governmental subvention administrated by the French National Research Agency (ANR) within the frame of the 'Future Investments' program (PIA), with the contractual reference 'ANR-11-EQPX-0037'. The Nord-Pas-de-Calais Region and the FEDER are thanked for their financialcontribution to the acquisition of the equipment of the platform.

Notes and references

[a] Institute of Condensed Matter and Nanosciences (IMCN), Université catholique de Louvain, Division Molecules, Solids and Reactivity (MOST), Croix du Sud 2 L7.05.15, 1348 Louvain la Neuve, Belgique.
[b] Univ. Lille Nord de France, F-59000, Lille, France
[c] Unité de Catalyse et de Chimie du Solide, UCCS (UMR CNRS 8181), Cité Scientifique, F-59650, Villeneuve d'Ascq, France
*corresponding author: robert.wojcieszak@univ-lille1.fr

1 Z. Yin, H. Zheng, D. Ma and X. Bao, *J. Phys. Chem. C,* 2009, **113 (3)**, 1001.
2 R. Wojcieszak, E.M. Gaigneaux and P. Ruiz, *ChemCatChem* 2013, **5**, 339.
3 R. Wojcieszak, R. Mateos-Blanco, D. Hauwaert, S.R.G. Carrazan, E. Gaigneaux and P. Ruiz, *Current Catal.* 2013, **2**, 27.
4 R. Wojcieszak, M.N. Ghazzal, E.M. Gaigneaux and P. Ruiz. *Catal. Sci. Tech*. 2014, **4(3)**, 738
5 G. Bonura, M. Cordaro, L. Spadaro, C. Cannilla, F. Arena and F. Frusteri, *Appl. Catal. B: Env*. 2013, **140-141**, 16.
6 J. Agrell, K. Hasselbo, S.G. Järas and M. Boutonnet, *Appl. Catal. A: Gen.* 2001, **211**, 239.
7 S. Velu, K. Suzuki, M. Okazaki, M.P. Kapoor, T. Osaki and F. Ohashi, *J. Catal.* 2000, **194**, 373.
8 S Murcia-Mascaros, R.M Navarro, L Gomez-Sainero, U Costantino, M Nocchetti and J.L.G Fierro, *J. Catal.* 2001, **198**, 338.
9 R. Zhang, Y-H. Sun and S. Peng, *React. Kinet. Katal. Lett.* 1999, **67**, 95.
10 C. Adami; M. Slany; J. Karl; G. Kaibel; M. Schäfer; P. Zehner and M. Röper; U.S. Patent No. 7,053,239; BASF Aktiengesellschaft, Ludwigshafen, DE, 2006.
11 H. Liu and E. Iglesia, *J. Phys. Chem. B* 2005, **109**, 2155.
12 J. Lichtenberger, D. Lee and E. Iglesia, *Phys. Chem. Chem. Phys*. 2007, **9**, 4902.
13 C. Louis, J.M. Tatibouët, M. Che, *J. Catal*. 1988, 109, 354
14 J.H. Scofield, *J. Electron Spectrosc. Relat. Phenom*. 1976, **8(2)**, 129
15 S.M. Davis, *J. Catal*. 1989, **117**, 432.
16 R.Wojcieszak, M. Genet, P. Eloy, P. Ruiz and E.M. Gaigneaux, *J. Phys. Chem. C* 2010, **114,** 16677.
17 M. Boutonnet, J. Kizling, P. Stenius and G. Maire, *Coll. Surf.* 1982, **5**, 209.
18 T. Hanaoka, T. Hatsuta, T. Tago, M. Kishida and K. Wakabayashi *Appl. Cata. A* 2000, **190**, 291.
19 V. Lochar, *Appl. Catal. A:* 2006, 309, 33.
20 V. Lochar, J. Machek and J. Tichý, *Appl. Catal. A:* 2002, 228, 95.
21 J. Liu, E. Zhan, W. Cai, J. Li and W. Shen, *Catal. Lett.* 2008, 120, 274.
22 O. Demoulin, M. Navez, E. M. Gaigneaux, P. Ruiz, A. S. Mamede, P. Granger and E. Payen, *Phys. Chem. Chem. Phys.* 2003, **5**, 4394.
23 J. M. Tatibouët, *Appl. Catal. A* 1997, **148**, 213.
24 E. Tronconi, A. S. Elmi, N. Ferlazzo, P. Forzatti, G. Busca and P. Tittarelli, *Ind. Eng. Chem. Res.* 1987, **26**, 1269.
25 M. Ai, *J. Catal.* 1982, **77**, 279.

26 S. A. Kirillov, P. E. Tsiakaras and I. V. Romanova, *J. Mol. Struct.* 2003, **651–653**, 365.
27 S. P. Bates, M. J. Gillan and G. Kresse, *J. Phys. Chem. B* 1998, **102**, 2017.
28 G. C. Cabilla, A. L. Bonivardi and M. A. Baltanás, *J. Catal.* 2001, **201**, 213.